Two-colour free electron laser with wide frequency separation using a single monoenergetic electron beam

Two-colour free electron laser with wide frequency separation using a single monoenergetic electron beam

L T Campbell[1,2,3,4]**, B W J McNeil**[3] **and S Reiche**[5]

[1] Center for Free-Electron Laser Science, Notkestrasse 85, Hamburg, Germany
[2] Institut für Experimentalphysik, Universität Hamburg, Hamburg, Germany
[3] SUPA, Department of Physics, University of Strathclyde, Glasgow, UK
[4] ASTeC, STFC Daresbury Laboratory and Cockcroft Institute, Warrington WA4 4AD, UK
[5] Paul Scherrer Institute, Villigen PSI, Switzerland
E-mail: lawrence.campbell@strath.ac.uk, b.w.j.mcneil@strath.ac.uk and sven.reiche@psi.ch

Abstract

Studies of a broad bandwidth, two-colour free electron laser (FEL) amplifier using one monoenergetic electron beam are presented. The two-colour FEL interaction is achieved using a series of undulator modules alternately tuned to two well-separated resonant frequencies. Using the broad bandwidth FEL simulation code Puffin, the electron beam is shown to bunch strongly and simultaneously at the two resonant frequencies. Electron bunching components are also generated at the sum and difference of the resonant frequencies.

Keywords: free electron laser, two-colour, single beam

1. Introduction

X-ray free electron lasers are now operating [1, 2] or under construction around the world [3]. These provide sources of high brightness, monochromatic x-rays that are driving forward many new scientific discoveries. There is now also increasing user interest in the simultaneous delivery of such radiation at two distinct colours, either simultaneously, or with a short time-delay in a pump-probe architecture.

Two colour operation of an FEL was first reported with a relatively low colour contrast in an infra-red oscillator configuration [4], with greater colour contrasts also possible [5]. More recently, two-colour operation has been achieved from the UV into the x-ray using different configurations of an FEL amplifier. For example, two-colour operation is being investigated using an electron beam composed of 'beamlets' of more than one energy [6–8]. These beamlets, typically of energy separation greater than the FEL amplification bandwidth, propagate through identical undulator modules and lase independently and simultaneously. If the higher energy beamlet emits at an harmonic of the lower energy, then coupling between the beamlets that is favourable to shorter wavelength generation can occur [9].

An alternative approach has been used in [10, 11] using a single monoenergetic electron beam propagating sequentially through two undulator modules each tuned to the two different colours. This method can generate two-colour radiation with a frequency separation of $\gtrsim 30\%$ [11]. In [12], a frequency separation of $\sim 4\%$ was demonstrated using an alternating series of undulator modules tuned to the two colours. This method generates radiation frequencies with a temporal overlap. In addition to the beating effects of the two resonant colours [8], a modal spectral structure [13] may arise due to the temporal shifts of each colour as it propagates non-resonantly over the electrons in alternate undulator modules.

Averaged FEL simulation codes such as [14–17] that make the slowly varying envelope approximation (SVEA) [18], can readily model two-colour FEL interactions when the radiation wavelengths are close to a fundamental frequency ω_1 and e.g. its third harmonic $\omega_3 = 3\omega_1$. This requires the radiation to be described by two distinct computational fields as the field sampling at any resonant radiation frequency ω_r means the frequency range able to be sampled is limited by the Nyquist condition to $\omega_r/2 < \omega < 3\omega_r/2$. Furthermore, the accuracy of the model decreases the further away from the resonant frequency. For a fundamental and e.g. its third harmonic field, the sampling can be over a common set of 'slices,' each an integer number of fundamental wavelengths in length.

However, for cases where the two frequencies in a two-colour FEL are strongly non-harmonic and well separated, e.g. where $\omega_2 = 0.417 \times \omega_1$, modelling of two computational fields using the averaged SVEA approximation becomes problematic: integer wavelength long slices of the two fields cannot be coincident and so when radiation propagation effects are modelled, electrons within these different length slices are driven asymmetrically in phase space leading to unphysical instabilities.

The unaveraged free electron laser simulation code Puffin [19] does not make the SVEA approximation and is therefore not restricted to the limited bandwidth of conventional averaged FEL codes. We therefore define such unaveraged simulation codes as being 'broad-bandwidth'. Furthermore, because Puffin also models the electron beam dynamics without averaging, the electrons are not confined to localized 'slices' of width the fundamental radiation wavelength, and a realistic electron beam interaction can occur over a broad bandwidth of radiation wavelengths. Puffin (along with other unaveraged codes e.g. [20–22, 23]) is then ideally suited to simulating and investigating the physics of multi-colour FELs.

In what follows, the Puffin code was modified to allow for undulator modules of different undulator parameters $\bar{a}_w$. This code was then used to simulate a high-gain two-colour FEL amplifier, with undulator modules alternately tuned to well separated, non-harmonic wavelengths. It is not immediately clear how such an interaction would be expected to progress and in particular how the electron phase space would develop when interacting resonantly with two distinct radiation wavelengths. The interaction is therefore first seeded,

rather than starting from noise, to allow a clearer picture of the electron beam and radiation evolution in the two-colour interaction. An example is then given of an unseeded, two-colour self amplified spontaneous emission (SASE)–FEL interaction.

2. Mathematical model

The resonant wavelength of the FEL interaction is given by [3]

$$\lambda = \frac{\lambda_w}{2\gamma_0^2}\left(1 + \bar{a}_w^2\right),\tag{1}$$

where $\bar{a}_w \propto B_w\lambda_w$ is the rms undulator parameter, B_w is the rms undulator magnetic field strength, λ_w is the undulator period and γ_0 is the initial electron beam Lorentz factor. Alternating the $\bar{a}_w$ of successive undulator modules, such as used in [12], generates the two resonant colours in the FEL interaction for a single monoenergetic electron beam. A variable undulator parameter is defined as $\bar{a}_w(\bar{z}) = \alpha(\bar{z})\bar{a}_{w1}$, where $\bar{a}_{w1}$ is a constant initial value.

Puffin uses a system of equations which utilizes scaled variables developed in [24]. These dimensionless variables are scaled with respect to the FEL parameter, defined as

$$\rho = \frac{1}{\gamma_0}\left(\frac{\bar{a}_w\omega_{\mathrm{p}}}{4ck_w}\right)^{2/3},\tag{2}$$

and $k_w = 2\pi/\lambda_w$. To model alternate undulator modules of different tuning, the modules are tuned by altering the rms undulator magnetic field only. A change in the tuning therefore also changes the FEL parameter, and so it is convenient to redefine the scaling used in Puffin to account for the different undulator tunings. The variable FEL parameter is then defined as:

$$\rho = \alpha^{2/3}\rho_1,\tag{3}$$

where ρ_1 is a constant using $\bar{a}_{w1}$ and the $\bar{z}$ dependence of α is understood. The electron beam focusing factor f of [19], is made variable to maintain a constant beam radius throughout different module tunings so that $f = \alpha f_1$. The Puffin equations can then be re-scaled with respect to the constant ρ_1 and $\bar{a}_{w1}$, making α explicit. The resulting equations are identical in form to equations (31–36) of [19], with the exception of two multiplicative factors of α in equations (32) and (33), which describe the evolution of the scaled transverse and longitudinal electron momentum $\bar{p}_\perp$ and p_2, respectively. Ignoring the explicit α scaling of the focusing terms f, these become

$$\frac{\mathrm{d}\bar{p}_{\perp j}}{\mathrm{d}\bar{z}} = \frac{1}{2\rho_1}\left[\mathrm{i}\alpha U^* - \frac{\eta p_{2j}}{f^2\bar{k}_\beta^2}A_{\perp j}\right]\tag{4}$$

$$\frac{\mathrm{d}p_{2j}}{\mathrm{d}\bar{z}} = \frac{2\rho_1}{u^2\eta}L_j^2\left[\eta p_{2j}\left(A_{\perp j}^*\bar{p}_{\perp j} + \mathrm{c.c.}\right)\right.$$
$$\left. - \mathrm{i}\alpha\left(1 + \eta p_{2j}\right)f^2\bar{k}_\beta^2\left(U\bar{p}_{\perp j} - \mathrm{c.c.}\right)\right],\tag{5}$$

where the scaled interaction length is $\bar{z} = z/l_{\mathrm{g}1}$ and $l_{\mathrm{g}1} = \lambda_w/4\pi\rho_1$ is the gain length of the $\alpha = 1$ interaction.
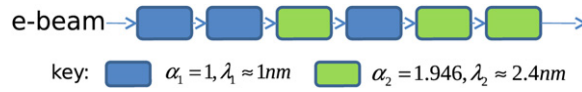
Figure 1. Modular undulator layout for well contrasted two-colour operation at wavelengths $\lambda_1 = 1$ nm and $\lambda_2 = 2.4$ nm.

The system of equations obtained is general, and α can be made any function of distance through the interaction as required. It could, for example, be used to taper the undulator in Puffin, or to provide any number of differently tuned undulator modules. For the purposes of this paper, α is varied between two values $\alpha_{1,2}$, corresponding to the two-colours of FEL radiation, $\omega_{1,2}$.

In the two-colour FEL, with only one resonant wavelength interaction occurring in each undulator module, radiation at the non-resonant wavelength will effectively propagate in free space. Two effects can be expected from this. Firstly, the non-resonant wavelength in an undulator module will undergo free-space diffraction (unless it is an harmonic when some guiding can occur [27]), which will reduce the net coupling of the radiation to the electron beam and so increase the effective gain length of the interaction for both colours. Secondly, the addition of extra relative slippage between the radiation and the electrons in the non-resonant undulator modules may reduce the radiation bandwidth [12, 25–28] and affect the spectrum by introducing modal effects [13], the latter being the subject of current study.

3. Simulation results

Simulations using this modified version of Puffin are now presented that model a two-colour FEL interaction using a single electron beam in sequential undulators tuned to two different resonant wavelengths. The first example is seeded by temporally coherent external laser sources at both of the resonant frequencies with intensities $\sim 10^{-4}$ less than the normal FEL saturation power. The seed powers are assumed constant over the duration of the electron pulse. These assumptions result in a simpler (cleaner) electron beam phase space from which the nature of the two-colour interaction is more easily observed. While such seeding is feasible at longer wavelengths, e.g. in the UV, it is not yet possible in the x-ray. Hence, the second example starts up from the electron beam shot-noise i.e. two-colour SASE to demonstrate x-ray operation. Radiation output spectra for differently tuned two-colour FELs are then summarized.

In a two-colour FEL, there will be a small drift section between each undulator module that may require radiation/electron beam phase matching using small tuning chicanes. Although Puffin is capable of modelling the drift sections none are modelled here and an instantaneous change in undulator parameter is applied. Puffin is also used here in the 1D limit as described in [19], so that simulations cost considerably less computational effort and the two-colour interaction can be observed in its simplest form. More detailed effects including diffraction, that can be expected to alter the optimum set-up, will be investigated in future work.

Modules with a fixed number of undulator periods are used which, while reflecting a probable experimental configuration, limits somewhat the options for driving both colours to the same powers. To compensate for the difference in gain lengths of the alternating modules ($l_{g2} = \alpha^{-2/3} l_{g1}$), the $N_m = 6$ undulator modules are arranged in the configuration of figure 1. This has a greater similarity to the configuration of [12], allowing both colours to experience gain

Table 1. Parameters for the two-colour simulations.

	Seeded	SASE	SASE scan
ρ	0.005	0.005	0.0011
γ_0	6316	6316	6900
σ_γ/γ_0	10^{-4}	10^{-4}	10^{-4}
$\bar{a}_{w0}$	1.0	1.0	1.2
N_{m}	6	8	10
N_w	25	25	100
α_1	1	1	1
α_2	1.946	1.946	scan

periodically through the interaction, and is unlike the configurations of [10, 11] which amplify each wavelength in two consecutive interactions.

The limit on the beam energy spread which must be satisfied for gain, $\Delta\gamma/\gamma_0 \lesssim \alpha^{2/3}\rho_1$, also approximates the energy spread at FEL saturation. The undulator configuration of figure 1 has modules resonant at the wavelengths [1, 1, 2, 1, 2, 2] and is chosen to avoid too much initial amplification of the longer wavelength. When the two-colours are well contrasted, as in the following simulations, the longer wavelength interaction could inflate the beam energy spread to impede the interaction at the shorter wavelength, which has the tighter energy spread constraint. For the same reason, it is preferable that the shorter wavelength is driven close to saturation prior to the longer and then ending the interaction at the longer wavelength.

The undulator module layouts in all of the following cases are designed with these arguments in mind, and are chosen to avoid full saturation of either colour. The post-saturation regime may be the subject of further publications.

3.1. Seeded example

The parameters for the first seeded case are shown in table 1. A small seed field is injected at each resonant frequency, and the electron beam has a 'flat-top' current profile. In the scaled frame $\bar{z}_2 = (ct - z)/l_{c1}$, where $l_{c1} = \lambda_1/4\pi\rho_1$ is the cooperation length [3] of the shorter wavelength, the scaled resonant frequencies $\bar{\omega} = \omega/2\rho\omega_1$ are $\bar{\omega}_1 = 100$ and $\bar{\omega}_2 \approx 41.7$. In addition to the scaled radiation field $A_\perp$ of [19], it is useful to define a measure of the spectral bunching of the N electrons as

$$\tilde{b}(\bar{z}, \bar{\omega}) = \frac{1}{\sqrt{2\pi}} \int_{-\infty}^{\infty} s(\bar{z}, \bar{z}_2) e^{-i\bar{\omega}\bar{z}_2} d\bar{z}_2 \tag{6}$$

where

$$s(\bar{z}, \bar{z}_2) = \frac{1}{\bar{n}_{\mathrm{p}}} \sum_{j=1}^{N} e^{-i\bar{z}/2\rho} \delta\left(\bar{z}_2 - \bar{z}_{2j}(\bar{z})\right), \tag{7}$$

is the source term of the unaveraged radiation wave equation in the Compton limit [19] for the α_1 undulator and $\bar{n}_{\mathrm{p}}$ is the peak linear density of electrons per unit $\bar{z}_2$.

Detail of the electron phase space and the modulus of the spectral bunching parameter is shown in figure 2 at the end of the third module, and still in the linear regime, where $\bar{z} \approx 4.71$.
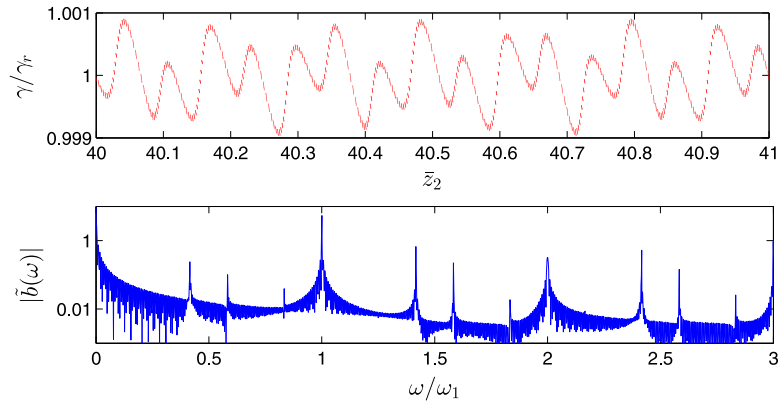
Figure 2. Electron parameters at output of third undulator module: detail of electron phase space between $40 < \bar{z}_2 < 41$ (top); and modulus of spectral bunching parameter $\tilde{b}(\bar{\omega})$ (bottom) at the output of the third undulator module at $\bar{z} = 4.71$.
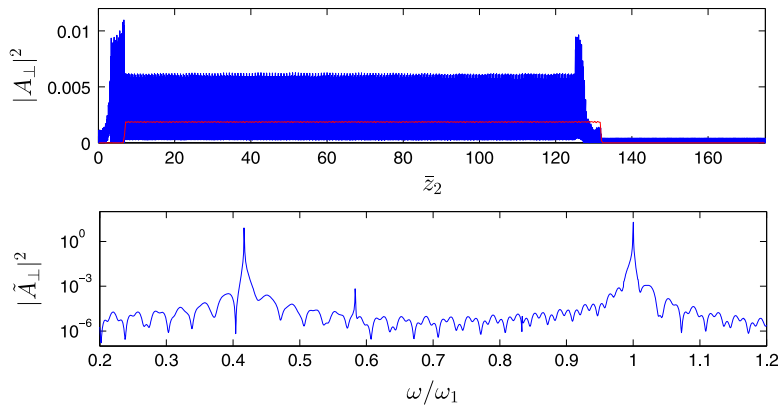

Figure 3. Scaled radiation intensity $|A_\perp|^2$ as a function of the scaled temporal coordinate $\bar{z}_2$ (top) and the scaled spectral intensity $|\tilde{A}_\perp|^2$ (bottom) at the output of the third undulator module at $\bar{z} = 4.71$. The red line in the temporal intensity plot indicates the current profile of the electron beam.

The bunching spectrum, shown in the bottom plot of figure 2, clearly shows bunching components at both frequencies, $\omega/\omega_1 = 1$ and 0.417. It is interesting to note here that the beam also displays bunching components at the harmonics and the sums and differences between all of these frequencies. In the beam phase space of the top plot, these bunching components are seen in the superimposed periodic electron modulations of periods in $\bar{z}_2$ of $\lambda_{1,2} = 4\pi\rho_1 \times \omega_1/\omega_{1,2} \approx 0.063$ and 0.15 respectively.

The corresponding scaled 'instantaneous' temporal intensity (i.e. including the fast oscillatory terms of the field [19]) and the scaled spectral intensity at the end of the third module are plotted in figure 3. The head of the electron pulse (shown in red in the top window) starts the beginning of the interaction at $\bar{z}_2 = 0$, and slips behind the radiation towards larger values of $\bar{z}_2 = \bar{z}$ as the interaction progresses through the undulator. Coherent spontaneous emission at the tail and head of the rectangular current distribution are visible in the top intensity plot. Detail of the spectrum in the bottom plot shows the strong emission at the resonant frequencies
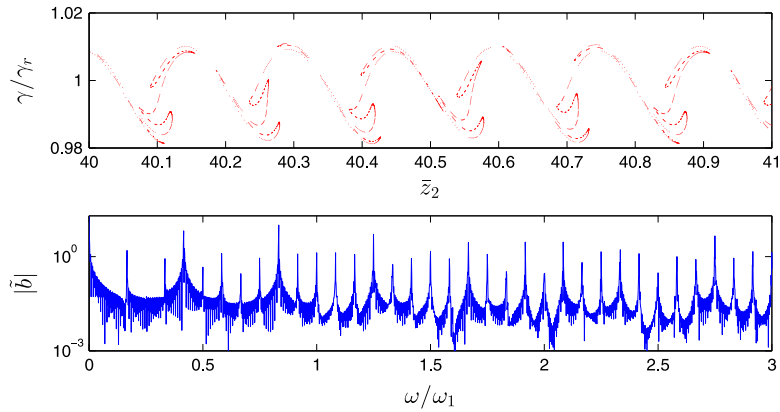
Figure 4. As figure 2 at output from sixth undulator module at $\bar{z} = 9.42$.
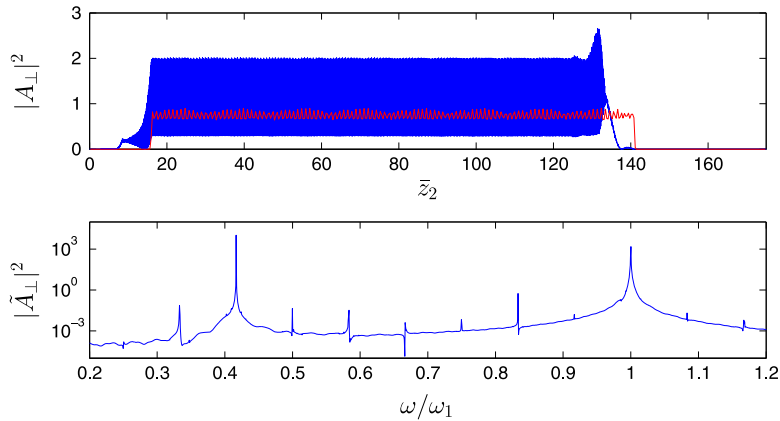

Figure 5. As figure 3 at output from sixth undulator module at $\bar{z} = 9.42$.

$\omega/\omega_1 = 1$ and 0.417, of the two undulator modules. A weaker emission is seen at the difference frequency $\omega/\omega_1 = 1 - 0.417 = 0.583$.

Figures 4 and 5 plot the same output at the end of the sixth undulator module at $\bar{z} = 9.42$, where the longer wavelength is close to saturation, slightly ahead of the shorter. A quite complex electron phase space has developed as a result of the two-colour interaction which has generated spectral intensities that are approximately equal for the two-colours.

The interaction at the longer wavelength λ_2 has a greater energy spread tolerance, so the energy modulations at λ_1 do not have as great an effect on the λ_2 interaction. Due to dispersion in non-resonant undulators, this can reduce bunching at the shorter wavelength λ_1 in regions where the energy modulation at λ_2 shifts the beam off-resonance. The resultant oscillation of the bunching at λ_1 therefore occurs with period λ_2, and consequently bunching is observed at the sum and difference frequencies $\omega_1 + \omega_2$ and $\omega_1 - \omega_2$.

This effect generates more frequency components in the bunching as the FEL process develops. As seen in figure 4, the same mechanism applies as the bunching at λ_2 and its harmonics grow, so that components develop not just at the sum and difference of the lasing frequencies, but also with the higher harmonic frequencies.
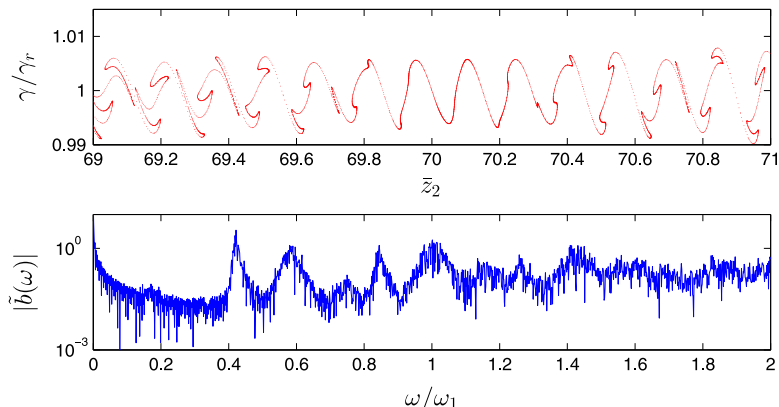
Figure 6. Electron parameters at output of ninth undulator module for SASE: detail of electron phase space between $69 < \bar{z}_2 < 71$ (top); and modulus of spectral bunching parameter $\tilde{b}(\bar{\omega})$ (bottom) at the output of the ninth undulator module at $\bar{z} = 14.12$.

3.2. Two-colour SASE example

The two-colour FEL interaction is now modelled starting from noise via SASE [24]. A similar, but extended, undulator beamline as that of figure 1 is used with $N_m = 9$ modules in a [1, 1, 2, 1, 1, 2, 1, 2, 2] configuration, to allow for a longer build-up from noise. Otherwise all parameters are identical to the previous seeded case.

One factor that is present in the two-colour SASE, that does not exist in the seeded case, is the potential for phase mis-matching between the radiation and the electron beam due to the extra induced slippage in the alternate non-resonant undulator modules. This may be mitigated by using modules $\lesssim 1$ gain length, ensuring relative slippages are not significantly longer than a cooperation length, so maintaining beam/radiation phase matching. While additional slippage may also assist in improving the coherence of the radiation field as discussed above, this should not significantly affect the results presented here.

As the system now starts from noise, the resultant beam phase space is less structured but maintains similar characteristics to the previous seeded simulations. Similarly to figure 4, the electron phase space close to saturation is seen from figure 6 to have bunching components at both resonant frequencies $\omega_{1,2}$ and at the sum and difference frequencies. The corresponding scaled radiation intensity and spectrum equivalent to the seeded case of figure 5 are plotted in figure 7, where the spectral intensity levels at both resonant frequencies are seen to be approximately equal. Unlike the seeded case, the temporal intensity has the familiar chaotic pulse structure.

Similar two-colour SASE simulations were also carried out for a system with a longer gain length more typical of an x-ray FEL, and with the electron beam and undulator parameters similar to the Athos FEL proposed at SwissFEL [29]. The FEL parameter is reduced to $\rho_1 = 0.001$, and the number of undulator periods per module has been increased to $N_w = 100$ to accomodate the longer gain length. There are now $N_m = 10$ modules in a [1, 1, 2, 1, 1, 2, 1, 1, 2, 2] configuration. Maintaining the same higher resonant wavelength of $\lambda_1 = 1$ nm for $\alpha_1 = 1$, simulations for two different two-colour configurations were carried out for $\lambda_2 = 2.7$ nm and $\lambda_2 = 3.8$ nm corresponding to $\alpha_2 = 1.95$ and 2.37 respectively. The normalized saturated SASE spectra (i.e. neglecting the strong CSE emitted
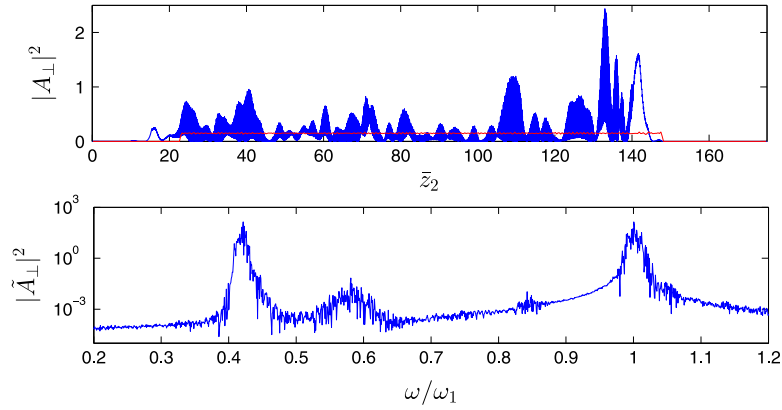
Figure 7. Scaled radiation SASE intensity $|A_\perp|^2$ as a function of the scaled temporal coordinate $\bar{z}_2$ (top) and the scaled spectral intensity $|\tilde{A}_\perp|^2$ (bottom) at the output of the ninth undulator module at $\bar{z} = 14.12$. The red line in the temporal intensity plot indicates the current profile of the electron beam.
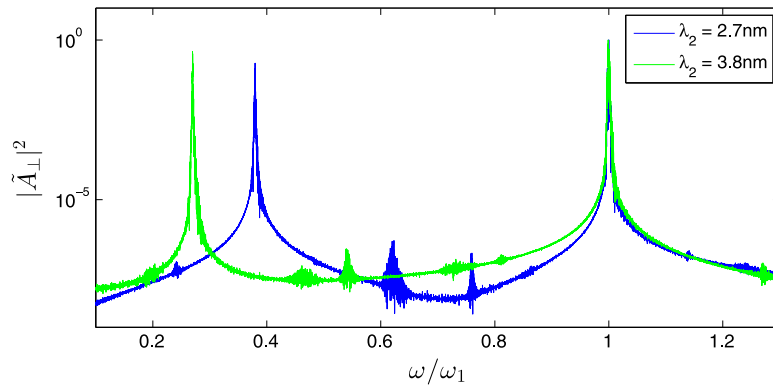

Figure 8. Scaled radiation intensity spectra at output for two different two-colour operating frequencies.

from the head and tail of the flat-top electron beam) of the scaled output intensities are plotted in figure 8 and demonstrates that the principle of such two-colour FEL operation applies across a wide range of wavelengths and to similar saturated radiation powers. No attempt has been made to optimize the output here, so that the output at a given wavelength may be improved upon. The statistical nature of the output is also unaccounted for in these single-shot simulations.

4. Conclusion

The principle of two-colour FEL amplifier lasing using a mono-energetic electron beam in a series of alternately tuned undulator modules was, for the first time, simulated at widely spaced, non-harmonic wavelengths. Such simulations are only practical using non-averaged, broad bandwidth FEL simulation codes such as Puffin [19]. To enable two-colour modelling, Puffin was modified from that described in [19] to allow for any general variation in the magnetic field strength along the undulator.

Both seeded and SASE two-colour operation were demonstrated to saturation and gave similar peak spectral intensities at both the resonant wavelengths. Such simultaneous FEL lasing to saturation by one electron beam at two distinct, harmonically uncoupled, wavelengths is perhaps not an immediately intuitive result. However, the electron phase-space evolution has a rich structure, including bunching at the sum and difference frequencies and harmonic components, that clearly demonstrates the simultaneous electron bunching and emission at the two distinct wavelengths. This result may open up other avenues for further research, for example in the generation of higher-modal radiation emission, multi-modal emission using multiply tuned undulator modules, or perhaps nonlinear frequency mixing processes in the FEL [8].

In the case of the two-colour SASE simulations, only a limited number of simulations were performed for each case so that the statistical nature of the two-colour processes were not explored. In both the seeded and SASE cases the scaled saturation variables indicates that parameters such as photon numbers and pulse durations will be similar to those for the equivalent single colour interaction.

Other factors must be taken into account in future 3D simulations. Diffraction will clearly have an effect during 'free' propagation of the radiation in the non-resonant undulator modules. Another factor is the transverse beam matching to different undulator modules. This could become more problematic for larger differences in $\bar{a}_w$ between undulator modules and may limit the range of the two-colour operation. Clearly, further examination in 3D is needed to identify and perhaps find solutions to such issues.

Acknowledgements

References

[1] Emma P *et al* 2010 *Nat. Photonics* **4** 641
[2] Ishikawa T *et al* 2012 *Nat. Photonics* **6** 540
[3] McNeil B W J and Thompson N R 2010 *Nat. Photonics* **4** 814
[4] Jaroszynski D A, Prazeres R, Glotin F and Ortega J M 1994 *Phys. Rev. Lett.* **72** 2387
[5] Krishnagopal S and Kumar V 1995 *Opt. Commun.* **119** 313–9
[6] Ronsivalle C *et al* 2014 *New J. Phys.* **16** 033018
[7] Petrillo V *et al* 2013 *Phys. Rev. Lett.* **111** 114802
[8] Ciocci F, Dattoli G, Pagnutti S, Petralia A, Sabia E, Ottaviani P L, Ferrario M, Villa F and Petrillo V 2013 *Phys. Rev. Lett.* **111** 264801
[9] McNeil B W J, Robb G R M and Poole M W 2004 *Phys. Rev. E* **70** 035501(R)
[10] Lutman A A, Coffee R, Ding Y, Huang Z, Krzywinski J, Maxwell T, Messerschmidt M and Nuhn H-D 2013 *Phys. Rev. Lett.* **110** 134801
[11] Hara T *et al* 2013 *Nat. Commun.* **4** 2919
[12] Marinelli A *et al* 2013 *Phys. Rev. Lett.* **111** 134801

[13] Thomson N R and McNeil B W J 2008 *Phys. Rev. Lett.* **100** 203901

[14] Freund H P 1995 *Phys. Rev.* E **52** 5401

[15] Reiche S 1999 *Nucl. Instrum. Methods Phys. Res.* A **429** 243–8

[16] Saldin E L, Schneidmiller E A and Yurkov M V 1999 *Nucl. Instrum. Methods Phys. Res.* A **429** 233–7

[17] Fawley W M 2006 *Proc. of FEL 2006* (Berlin: BESSY) pp 218–21

[18] Arecchi F T and Bonifacio R 1965 *IEEE J. Quantum Electron.* **QE-1** 169

[19] Campbell L T and McNeil B W J 2012 *Phys. Plasmas* **19** 093119

[20] Piovella N 1999 *Phys. Plasmas* **6** 3358

[21] McNeil B W J, Robb G R M and Jaroszynski D A 1999 *Opt. Commun.* **165** 65

[22] Bajlekov S I, Hooker S M and Bartolini R 2009 *Proc. FEL (Liverpool, 2009)* MOPC42

[23] Maroli C, Petrillo V and Ferrario M 2011 *Phys. Rev. ST Accel. Beams* **14** 070703

[24] Bonifacio R, Pellegrini C and Narducci L M 1984 *Opt. Commun.* **50** 373

[25] Thompson N R, Dunning D J and McNeil B W J 2010 *Proc. IPAC10 (Kyoto)* p TUPE050

[26] Wu J, Marinelli A and Pellegrini C 2012 *Proc. FEL (Nara)* p TUPD07

[27] Xiang D, Ding Y, Huang Z and Deng H 2013 *Phys. Rev. ST Accel. Beams* **16** 010703

[28] McNeil B W J, Thompson N R and Dunning D J 2013 *Phys. Rev. Lett.* **110** 134802

[29] Ganter R (ed) 2012 *SwissFEL Conceptual Design Report* (*PSI Bericht Nr. 10-04*)